

Single- and Two-Photon Spectral Imaging of Intrinsic Fluorescence of Transformed Human Hepatocytes

BARTEK RAJWA,^{1*} TYTUS BERNAS,^{2,3} HELMUT ACKER,⁴ JUREK DOBRUCKI,⁵ AND J.P. ROBINSON^{1,2}

¹Purdue University Cytometry Laboratories, Bindley Bioscience Center, Purdue University, West Lafayette, Indiana 47907-2057

²School of Veterinary Medicine, Purdue University, West Lafayette, Indiana 47907-2026

³Department of Plant Anatomy and Cytology, Faculty of Biology and Protection of Environment, Katowice, Poland

⁴Institut für Physiologie, Universitätsklinikum Essen, D - 45147 Essen, Germany

⁵Division of Cell Biophysics, Faculty of Biochemistry, Biophysics and Biotechnology, Jagiellonian University, 30-387 Krakow, Poland

KEY WORDS autofluorescence; confocal microscopy; 2-photon microscopy; spectral imaging

ABSTRACT Autofluorescence (AF) originating from the cytoplasmic region of mammalian cells has been thoroughly investigated; however, AF from plasma membranes of viable intact cells is less well known, and has been mentioned only in a few older publications. Herein, we report results describing single- and two-photon spectral properties of a strong yellowish-green AF confined to the plasma-membrane region of transformed human hepatocytes (HepG2) grown in vitro as small three-dimensional aggregates or as monolayers. The excitation–emission characteristics of the membrane AF indicate that it may originate from a flavin derivative. Furthermore, the AF was closely associated with the plasma membranes of HepG2 cells, and its presence and intensity were dependent on cell metabolic state, membrane integrity and presence of reducing agents. This AF could be detected both in live intact cells and in formaldehyde-fixed cells. *Microsc. Res. Tech.* 70:869–879, 2007. © 2007 Wiley-Liss, Inc.

INTRODUCTION

Endogenous fluorochromes may impede image or flow cytometry studies of mammalian cells. However, autofluorescence (AF) may carry useful biological information as well. AF of NAD(P)H and lipoamine dehydrogenase has been applied to probe the redox state of mitochondria in cells using fluorometry (Croce et al., 2004) and microfluorimetry (Eng et al., 1989; Huang et al., 2002; Patterson et al., 2000; Rocheleau et al., 2002, 2004). AF of intracellular flavins was used to study cell redox state with a flow cytometer (Thorell, 1983) and to establish subcellular localization of flavoproteins using microscope imaging (Masters and Chance, 1999). Moreover, tissues and whole organs have been studied using NADH-fluorescence imaging (Bennett et al., 1996; Kuznetsov et al., 1998; Piston et al., 1995; Puppels et al., 1999). Furthermore, FAD fluorescence has been used for identification and cell sorting of eosinophils and neutrophils (Watt et al., 1980; Weil and Chused, 1981). For these reasons, studies of cell AF are considered an interesting tool for analyzing intracellular physiopathological processes (Brookner et al., 2000; Dellinger et al., 1998; Huang et al., 2004; Kara et al., 2004; Plettenberg and Hoffmann, 2002).

Apart from reduced nicotinamide nucleotides (NADH, NADPH), oxidized flavin nucleotides (FAD, FMN) and endogenous fluorophores include lipofuscins, porphyrins, and a number of less abundant fluorophores (Croce et al., 2004). Their fluorescence has usually been detected throughout the cytoplasm (Andersson et al., 1998), or localized within the mito-

chondria (Patterson et al., 2000; Rocheleau et al., 2002, 2004) or cytoplasmic granules (Croce et al., 1999, 2004; Mayeno et al., 1992).

Although AF originating from the cytoplasmic region of mammalian cells has been studied by many researchers (Andersson et al., 1998; Aubin, 1979; Benson et al., 1979; Bondza-Kibangou et al., 2001; Croce et al., 1999; DaCosta et al., 2005; Georgakoudi et al., 2002; Matsui et al., 1998; Mayeno et al., 1992; Reinert et al., 2004), AF from plasma membranes of viable intact cells, less known and not thoroughly investigated, has been mentioned only in a few older reports (Lowy and Spring, 1990; Nokubo et al., 1988, 1989). These early reports did not provide detailed information about the spectral properties of the described AF. However, the authors suggested that AF was due to the presence of riboflavin associated with plasma membranes. Since little is known about the role of free riboflavin in cellular plasma membranes, this controversial hypothesis has never been widely accepted.

*Correspondence to: Bartek Rajwa, Purdue University Cytometry Laboratories, Bindley Bioscience Center, 1203 W. State Street, West Lafayette, Indiana 47907-2057, USA. E-mail: brajwa@purdue.edu

Received 18 August 2006; accepted in revised form 26 December 2006

Contract grant sponsor: Polish State Committee for Science; Contract grant numbers: KBN 2224/4/91, KBN 6P04A03912; Contract grant sponsor: Foundation for German-Polish Cooperation, Warsaw; Contract grant number: FWP 994/94; Contract grant sponsor: Jagiellonian University; Contract grant number: BW/99.

DOI 10.1002/jemt.20497

Published online 27 July 2007 in Wiley InterScience (www.interscience.wiley.com).

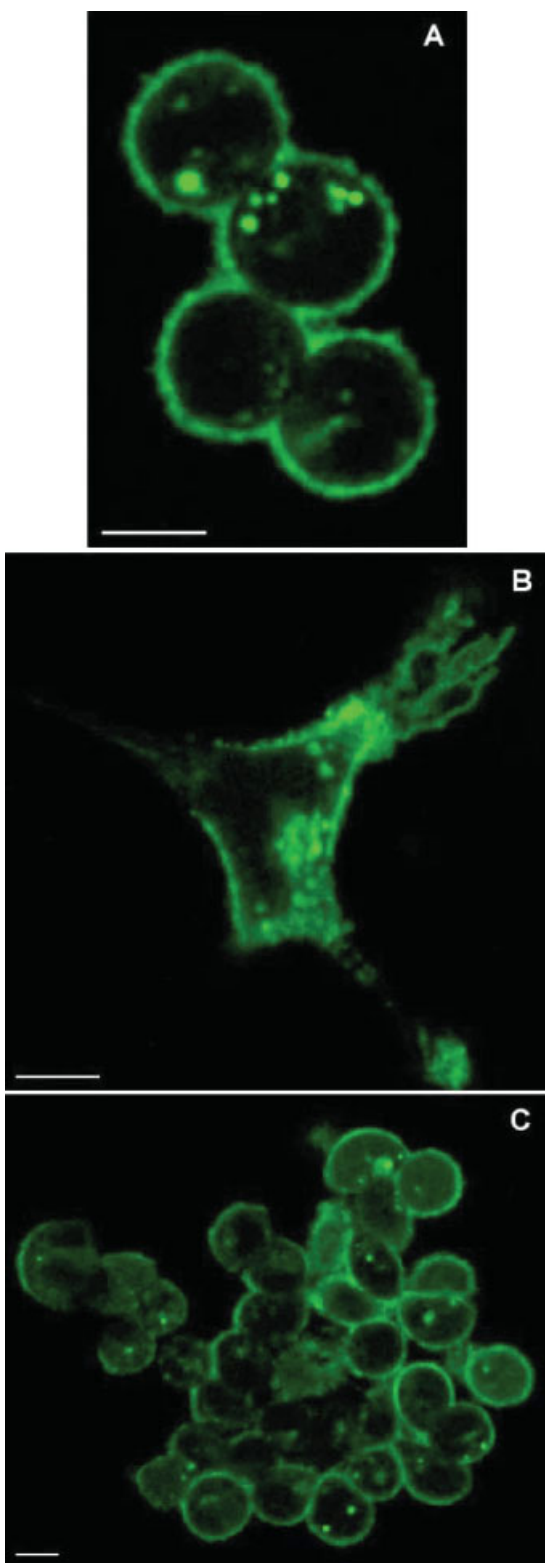


Fig. 1. Green autofluorescence of HepG2 human hepatoma grown in optimal conditions as single cells or as small aggregates in suspension (A), as monolayers (B), and as large cellular aggregates (C). Bar: 10 μm . [Color figure can be viewed in the online issue, which is available at www.interscience.wiley.com.]

We report here results describing spectral characteristics of a strong yellowish-green AF confined to the plasma-membrane region of transformed human hepatocytes (HepG2) grown in vitro as small three-dimensional aggregates or as monolayers. The AF excitation/emission spectrum was similar to that of free flavin. Furthermore, the AF was closely associated with the HepG2 plasma membranes, and its presence and intensity were dependent on cell metabolic state, membrane integrity, and presence of reducing agents. This AF could be detected both in live intact cells and in formaldehyde-fixed cells.

MATERIALS AND METHODS

Reagents

Digitonin was obtained from Sigma (MO). The solutions were made immediately prior to experiments. DiIC18 and riboflavin were obtained from Molecular Probes (OR).

Cell Cultures

HepG2 human hepatoma monolayers (ATCC, VA) and small-sized cellular aggregates were grown in DMEM (Sigma) supplemented with 2 mM L-glutamine, 100 units/mL penicillin, streptomycin (0.1 mg/mL), 10% fetal bovine serum, and phenol red.

In order to prepare cellular aggregates, cells were transferred onto Petri dishes containing agarose gel supplemented with medium. The dishes were incubated 72 h at 37°C in a humidified atmosphere containing 5% CO₂.

Four hours prior to experiments, cell aggregates were transferred onto 0.17-mm coverglasses and kept in HEPES-buffered DMEM without phenol red or in PBS. Coverglasses with cells attached to the substratum were mounted in a microincubator chamber (Life Science Research, Cambridge, UK), and 1 mL of DMEM without phenol red or 1 mL PBS was added. Live cells were imaged at a temperature of 37°C. Where indicated, the cells were fixed on the coverslips with 3% formaldehyde (in PBS) for 20 min and washed two times with PBS prior to imaging. Fixed cells were imaged at room temperature.

Confocal Microscopy

Confocal laser scanning microscopy was performed with a BioRad MRC1024 system based on an inverted Nikon Diaphot 300 microscope (Nikon, Japan). The system was equipped with a 60 \times PlanApo 1.4-NA oil-immersion objective lens, 100-mW argon-ion laser (ILT), three fluorescence detectors (PMTs), and a three-color transmitted nonconfocal light detector. Cells were illuminated with 457-nm light, using either a 510-nm dichroic long-pass filter (VHS BioRad filter block) or a 495-nm dichroic long-pass filter (custom-built filter block). AF was detected in the range of 490–550 nm using a 565-nm dichroic long-pass filter (A2 BioRad filter block) and a 522/35 band-pass filter (Chroma, VT). Where indicated, fluorescence of DiIC18 was registered in the range of 550–640 nm using a 550-nm long-pass filter (BioRad OG550). Images 512 \times 512 pixels in size (pixel size 0.135 μm) were registered in photon-counting mode (eight-bit dynamic range) using LaserSharp 3.2 software (Bio-Rad).

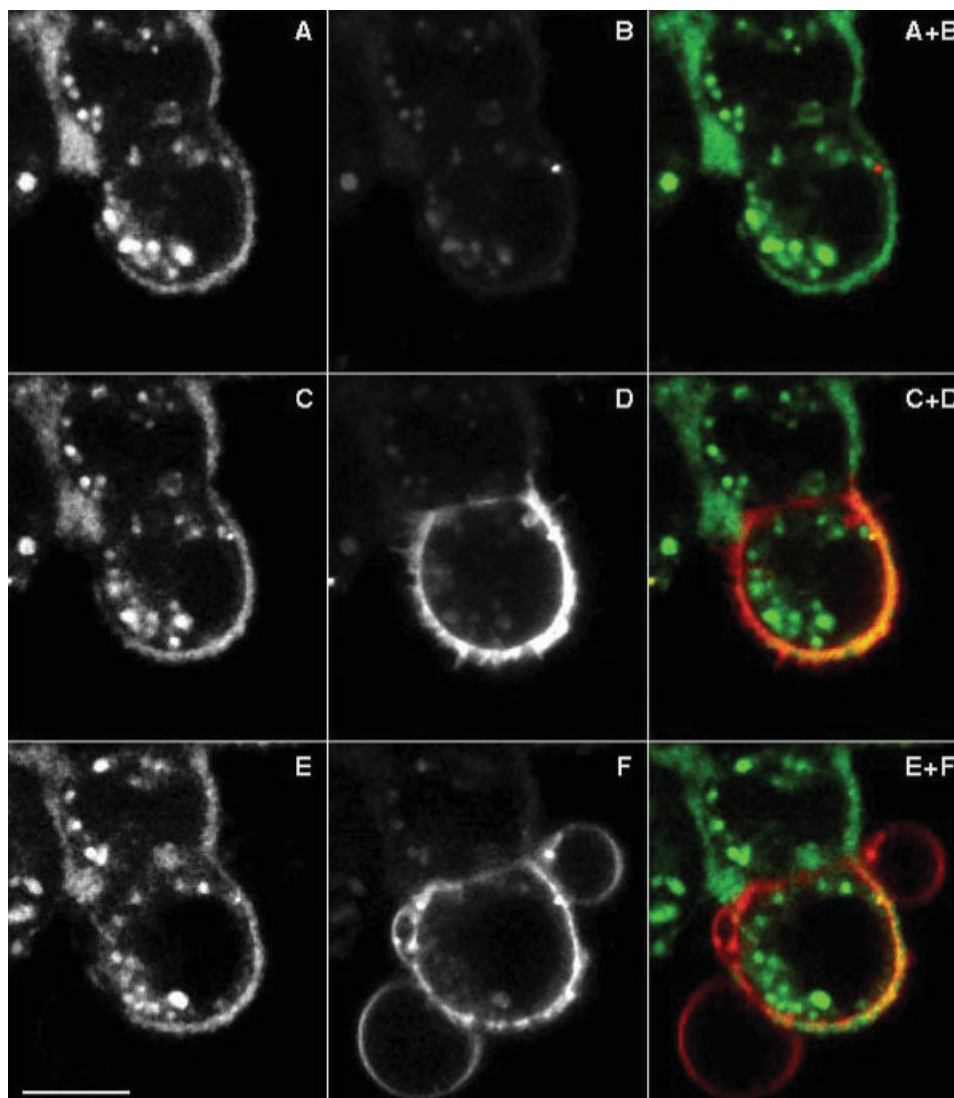


Fig. 2. Subcellular localization of green autofluorescence. Green (A) and red (B) AF of intact HepG2 cells, grown as small aggregates, prior to staining with DiIC18, immediately (4 min) following staining of a plasma membrane of one cell with DiIC18 (C and D), and 20 min later when blebs were formed (E and F). Bar: 10 μ m. [Color figure can be viewed in the online issue, which is available at www.interscience.wiley.com.]

Two-Photon Microscopy

Two-photon microscopy was performed using a BioRad Radiance 2100MP system based on an inverted Nikon Eclipse T2000-U microscope (Nikon). The system was equipped with a 40×1.2 -NA NeoFluor oil-immersion objective lens and a 1.5-W (at 800 nm) Mai Tai Titanium:Sapphire tunable (720–900 nm) impulse (100 fs) laser (Spectraphysics, USA), a 100-mW argon-ion laser (ILT), three point fluorescence detectors (conventional PMTs), and a direct fluorescence detection module (BioRad) comprising two array detectors (multicathode channel plate PMTs, Hamamatsu, Japan). Furthermore, the system was equipped with a three-color transmitted nonconfocal light detector. Cellular AF was excited using 720-, 765-, 810-, 855-, or 900-nm light. Images 512×512 pixels in size (pixel size 0.17 μ m) were registered in photon-counting mode (8- or 16-bit dynamic range). The point-scanning PMTs were controlled using a standard BioRad frame grabber and LaserSharp 2000 software. AF was registered using 500-nm and 560-nm dichroic low-pass mirrors (DCLPXR, Chroma) to direct the light

to the three PMTs, each equipped with a combination of a low-pass and a high-pass filter to provide detection in 30-nm wide bands. The AF spectrum comprised six such bands: 420–470 nm (1 - violet), 470–500 nm (2 - blue), 500–530 nm (3 - green), 530–560 nm (4 - orange), 590–620 nm (5 - red), 620–650 nm (6 - far red). Alternatively, a 500-nm dichroic low-pass mirror (DCLPXR, Chroma) and two direct detectors, controlled using an SPC 830 time-correlated single-photon counting module (Becker and Hickl, Germany), were used to collect autofluorescence in 400- to 490-nm and 500- to 560-nm bands set with appropriate band-pass filters (Chroma). In addition, transmitted-light (488-nm) images were collected after the fluorescence measurement. The emission spectrum of tubulin in fixed cells immunostained with fluorescein-labeled antibodies and excited by 860-nm light was used as the reference.

Microfluorimetry

High-resolution fluorescence emission spectra were measured using a Nikon Optiphot-2 wide-field micro-

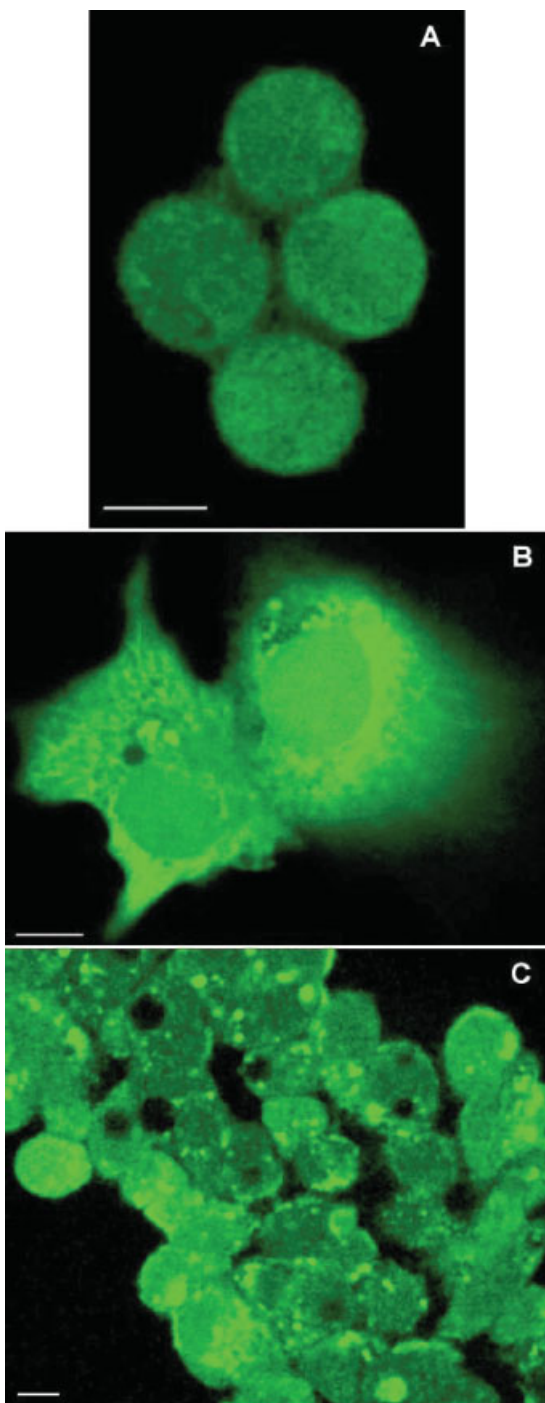


Fig. 3. Green autofluorescence of HepG2 human hepatoma grown in suboptimal conditions as single cells or as small aggregates in suspension (A), as monolayers (B), and as large cellular aggregates (C). Bar: 10 μm . [Color figure can be viewed in the online issue, which is available at www.interscience.wiley.com.]

scope (Nikon) equipped with a $40 \times 1.2\text{-NA}$ Fluor oil-immersion objective. Fluorescence was excited using a 100-W Hg arc lamp, and a 350–380-nm band-pass filter and a 405-nm long-pass dichroic mirror. Fluorescence was registered using an acousto-optical tunable filter MIM200 AOTF (Brimrose, MD). The emission was

measured from 450 to 710 nm in bands, which ranged in width from 3 nm (at 450 nm) to 6 nm (at 710 nm). A cooled CCD Rollera XR camera based on a VQE3618L Sony chip (Qimaging, Canada) was used to collect 348×260 images (2×2 binning). Effective pixel size in the image space was 0.64 μm . The emission spectrum of DAPI bound to DNA in nuclei of fixed cells was used as the reference.

Microinjection and Membrane Damage

Microinjection of the plasma membrane dye DiIC18 was performed using an Eppendorf Micromanipulator 5172 (Eppendorf, Germany). The plasma membrane of a single cell was stained by microinjecting 1 fL of DiIC18 in the immediate vicinity of that cell. The manipulator was employed to puncture the plasma membrane using a micropipette needle. Alternatively, digitonin (0.05 mM) was used to cause membrane damage. Integrity of plasma membranes was monitored using a propidium-iodide (PI) exclusion test. PI was added to cell cultures at a final concentration of 5 $\mu\text{g}/\text{mL}$. Red fluorescence from nuclei of damaged cells was detected by confocal microscopy.

Image Processing and Analysis

Intensity of fluorescence at the plasma membranes, in the cytoplasm, and in the cell nuclei was measured as described by Bernas and Dobrucki (1999). Briefly, for every cell present in the image, three types of regions of interest (ROIs) were chosen (using a transmitted-light image): ROIs containing no cells (so that all the signal in a ROI may be treated as background), ROIs enclosing only cytoplasm or a nucleus (cell interiors), and ROIs enclosing plasma membranes (i.e., the area contained within $\sim 0.5 \mu\text{m}$ of the edge of cell). The brightness threshold was chosen so that 95% of pixels in the background region were of lower or equal brightness. Fluorescence intensities at the membranes, in the nuclei, and in the cytoplasm were represented as averages of the pixels above threshold in the respective ROIs.

RESULTS

Subcellular Localization of AF

HepG2 human hepatoma cells exhibited yellowish-green (490–550-nm) AF under visible-light (457-nm) single-photon excitation, as depicted in Figure 1. Spatial distribution of AF was not uniform. Prominent AF was detected in the regions adjacent to cell edges. On the other hand, little AF was observed in cell nuclei and in the bulk of the cytoplasm. Emission from cytoplasm was concentrated in small ($\sim 1 \mu\text{m}$) granules. One should note a similar distribution of the cells grown as small cell aggregates in suspension (Fig. 1A), monolayers (Fig. 1B), or large cell aggregates (Fig. 1C).

To establish subcellular localization of AF we investigated the localization of the green AF and the plasma membrane tracer DiIC18 in HepG2 cells *in vitro*. The images in Figure 2 represent green and red fluorescence before (A, B) and after staining (CD and EF) of plasma membranes with the red-emitting dye DiIC18. The intensity of green AF was unaffected by injection of the membrane tracer. The dye did not diffuse into the plasma membrane of the neighboring cell. Merging of images from red and green channels confirmed colocalization between green AF and plasma membranes.

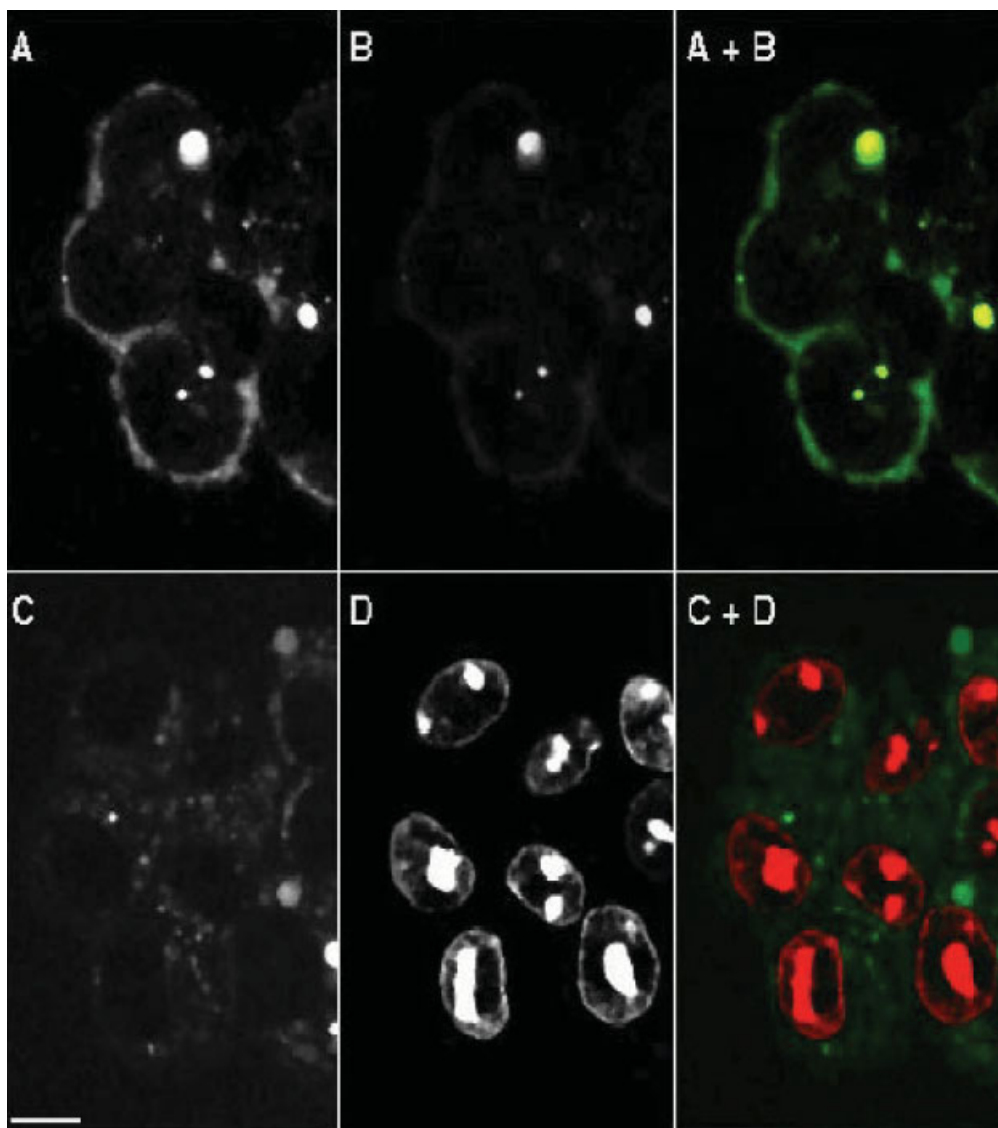


Fig. 4. Fluorescence of HepG2 cells before (A, B) and after digitonin treatment (C, D). Green channel (A, C) represents green AF (490–550 nm); red channel (B), weak red AF (585–630 nm), and fluorescence of nuclei stained with propidium iodide (D). Bar: 10 μ m. [Color figure can be viewed in the online issue, which is available at www.interscience.wiley.com.]

The presence of DiIC18 in the plasma membranes resulted eventually in the formation of membrane blebs (Fig. 2F). It is interesting to note that green AF was absent in the regions of membrane blebs. Apparently the fluorochrome responsible for green AF did not have the ability to diffuse laterally at the rapid rate characteristic for DiIC18. In order to verify this hypothesis, small regions in the plasma membranes were subjected to intense illumination with a 457-nm laser beam, which resulted in elimination (photobleaching) of the green AF in these regions. There was no observed recovery of fluorescence in photobleached regions of the plasma membrane. These results support the notion that the fluorophore is part of a protein complex, which in turn is anchored to the cytoskeleton.

HepG2 cells maintained under suboptimal growth conditions (i.e., without replenishing the medium for 48 h) exhibited different pattern of subcellular AF distribution (compare Figs. 1 and 3). Uniform AF distribution was detected for small aggregates in suspension (Fig. 3A), whereas cells grown as monolayers or as large aggregates exhibited strong granular fluorescence from the cytoplasm (Figs. 3B and 3C). The intensity of plasma-membrane AF increased and of cytoplasmic AF decreased again, following fresh medium replenishment (measured after 24 h). A similar change in subcellular distribution of AF followed the loss of plasma-membrane integrity in cells treated with digitonin (Fig. 4). One should note that whereas decrease of plasma-membrane AF was permanent, an increase of cytoplasmic AF was only transient. Loss of plasma-

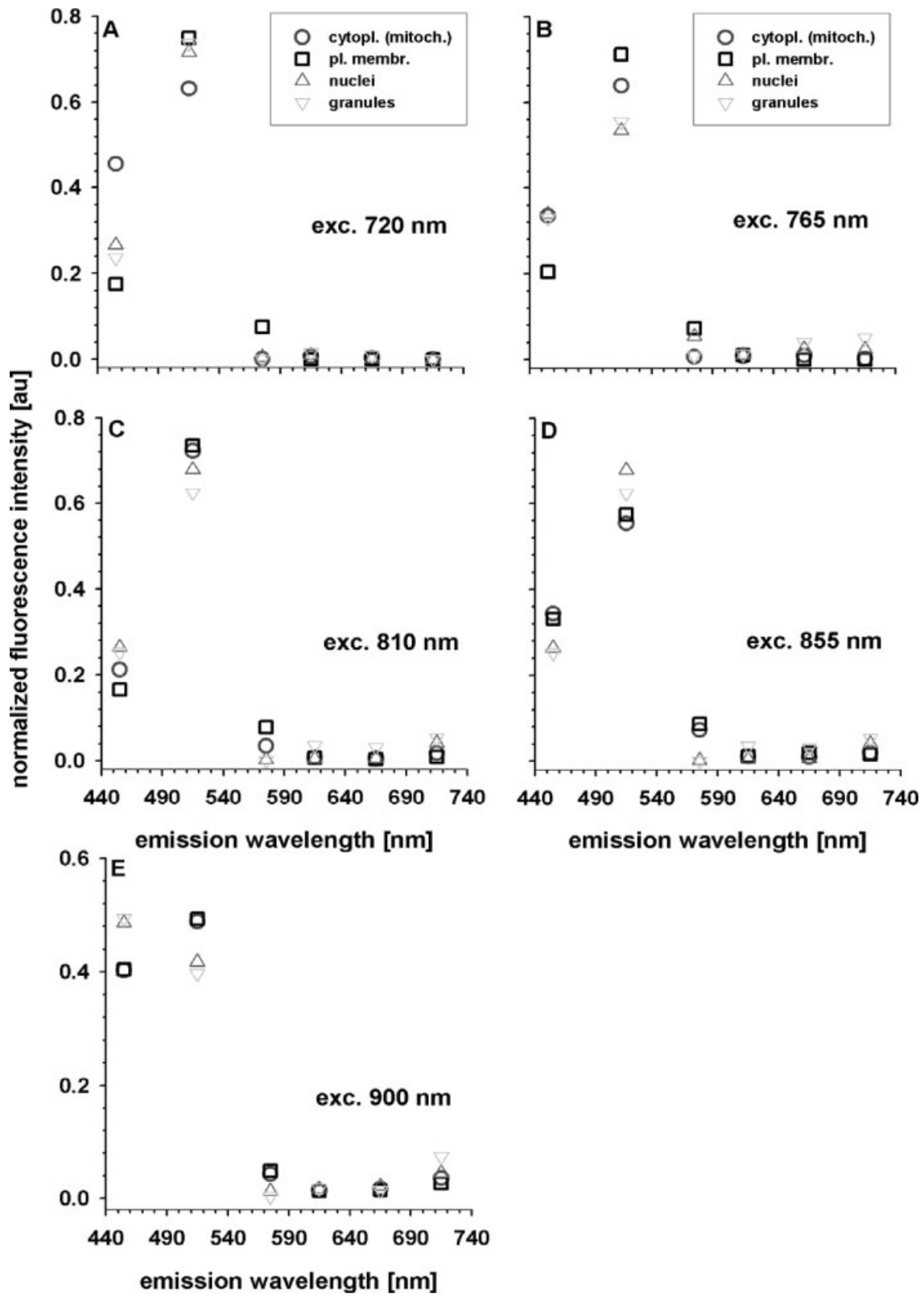


Fig. 5. Excitation/emission spectrum of autofluorescence (AF) of HepG2 cells. AF was excited in two-photon mode using 720- (A), 765- (B), 810- (C), 855- (D), and 900-nm (E) light. The detection bands were the following: 420–470 nm (1 - violet), 470–500 nm (2 - blue), 500–530 nm (3 - green), 530–560 nm (4 - orange), 590–620 nm (5 -

red), 620–650 nm (6 - far red). The AF intensity (z -axis) was measured in photon-counting mode at the plasma membrane (squares), in the cytoplasm (circles), in the cell nuclei (triangles up), and in the granules (triangles down).

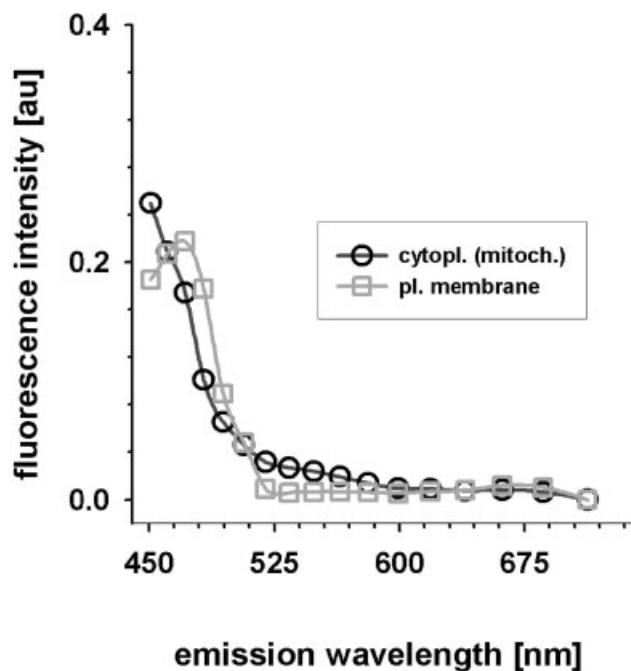


Fig. 6. Narrow-band emission spectrum of the autofluorescence (AF). The AF was excited using 350- to 380-nm light and detected in the range of 450–710 nm in 3-nm (at 450 nm) to 6-nm (at 710 nm) bands. The AF was registered at the plasma membrane (gray symbols) and in the cytoplasm (black symbols) of HepG2 cells.

membrane AF was also observed when a suspension of HepG2 cells was frozen in liquid nitrogen and thawed, or when the plasma membrane was mechanically punctured with a micropipette (data not shown).

One may conclude that plasma-membrane AF was dependent on the membrane integrity and on an optimal supply of nutrients during cell growth. Hence, further studies focused on cells with intact plasma membranes and cultured under optimal conditions.

Spectral Properties

Yellowish-green emission (490–550 nm) was the main component of cell AF excited by 457-nm light. Furthermore, weak red fluorescence (585–630 nm) was detectable at the plasma membranes when 457-nm or 568-nm light was used. No measurable AF in plasma membranes was observed with red-light (647-nm) excitation. Hence, two-photon excitation (equivalent to 350–450-nm one-photon) was used to characterize spectral properties of HepG2 AF (Fig. 5). The majority of AF emission at the plasma membranes (squares), in the cytoplasm (circles), in the nuclei (triangles up), and in the granules (triangles down) occurred in two bands: 420–470 nm (violet) and 470–500 nm (blue). This was true for all excitation wavelengths used. Minor AF was detectable in the green (500–530 nm) emission band at the plasma membrane and in the nuclei. One should note, however, that with 720-nm excitation AF of the plasma membranes was more prominent at longer (blue and green) wavelengths than AF in the cytoplasm (Fig. 5A). This difference decreased with increasing excitation wavelength (compare Figs. 5A–5E) and was negligible when 900-nm light was used for AF excita-

tion. Emission spectra of cytoplasm and nuclei were similar at all excitation wavelengths, whereas granules exhibited stronger AF in the range of 550–650 nm than did other cell compartments. One may postulate that only one kind of fluorochrome contributed to AF of the plasma membranes. On the other hand, it seems plausible that mitochondrial AF originated from more than one fluorochrome type. Hence, the fluorescence of plasma membranes and cytoplasm (mitochondria) was further characterized using microfluorimetry (see Materials and Methods). The emission spectra of the plasma-membrane fluorescence excited with UV are compatible with a flavin fluorochrome (Fig. 6). On the other hand, cytoplasmic fluorescence was blueshifted with respect to the typical flavin spectrum. One may conclude that the emission/excitation characteristics of plasma membrane AF corresponded to that of a flavin derivative, whereas mitochondrial AF might be a superposition of flavin and NAD(P)H emissions.

Effect of Free Riboflavin

It has been previously suggested that the fluorophore responsible for membrane AF was riboflavin transported to cells (Lowy and Spring, 1990). In order to verify that hypothesis, we altered riboflavin availability in the culture medium. Three hours of incubation in the presence of 10 $\mu\text{g}/\text{mL}$ of riboflavin-binding protein (RBP) in the culture medium did not decrease intensity of green AF (490–550 nm) observed with 457-nm excitation. One should note that the concentration of RBP was sufficient to complex all riboflavins present. On the other hand, a slight increase of violet/blue (400–490 nm) and green (500–560 nm) plasma-membrane AF was detectable with long-wave 2P excitation (810–900 nm) if 1 $\mu\text{g}/\text{mL}$ of riboflavin was added to the incubation medium (PBS, Figs. 7C and 7D). However, a concomitant slight decrease of violet/blue AF was observed in mitochondria (Fig. 7A) and cell nuclei (Fig. 7E) under short-wave 2P excitation (700–765 nm), whereas the green AF in these compartments did not change. These results appear incompatible with riboflavin transport from the extracellular environment (culture medium) to the interior of cells. Instead, one may postulate that free riboflavin acted as an electron acceptor, causing oxidation of flavins and NAD(P)H in cells. To test this hypothesis we examined the influence of reducing and oxidizing agents and of oxygen pressure on AF.

Redox Properties

Incubation of HepG2 cells with an exogenous electron acceptor, tetrazolium salt CTC, resulted in a gradual increase of yellowish-green (490–550 nm) AF at the plasma membranes (Figs. 8A–8E), registered using 457-nm excitation. A concomitant increase of red fluorescence (685–600 nm) was observed as well at the plasma membranes (Figs. 8B, 8D, and 8F). No changes of either red or green fluorescence in cellular interiors were detected. One should note that nonfluorescent CTC is water soluble and forms fluorescent deposits of CTC-formazan upon reduction. Hence, these results are consistent with CTCs being reduced at the plasma membranes, as reported previously (Bernas and Dobrucki, 1999). Exposure to hypoxia and then reexposure to atmospheric oxygen did not change the inten-

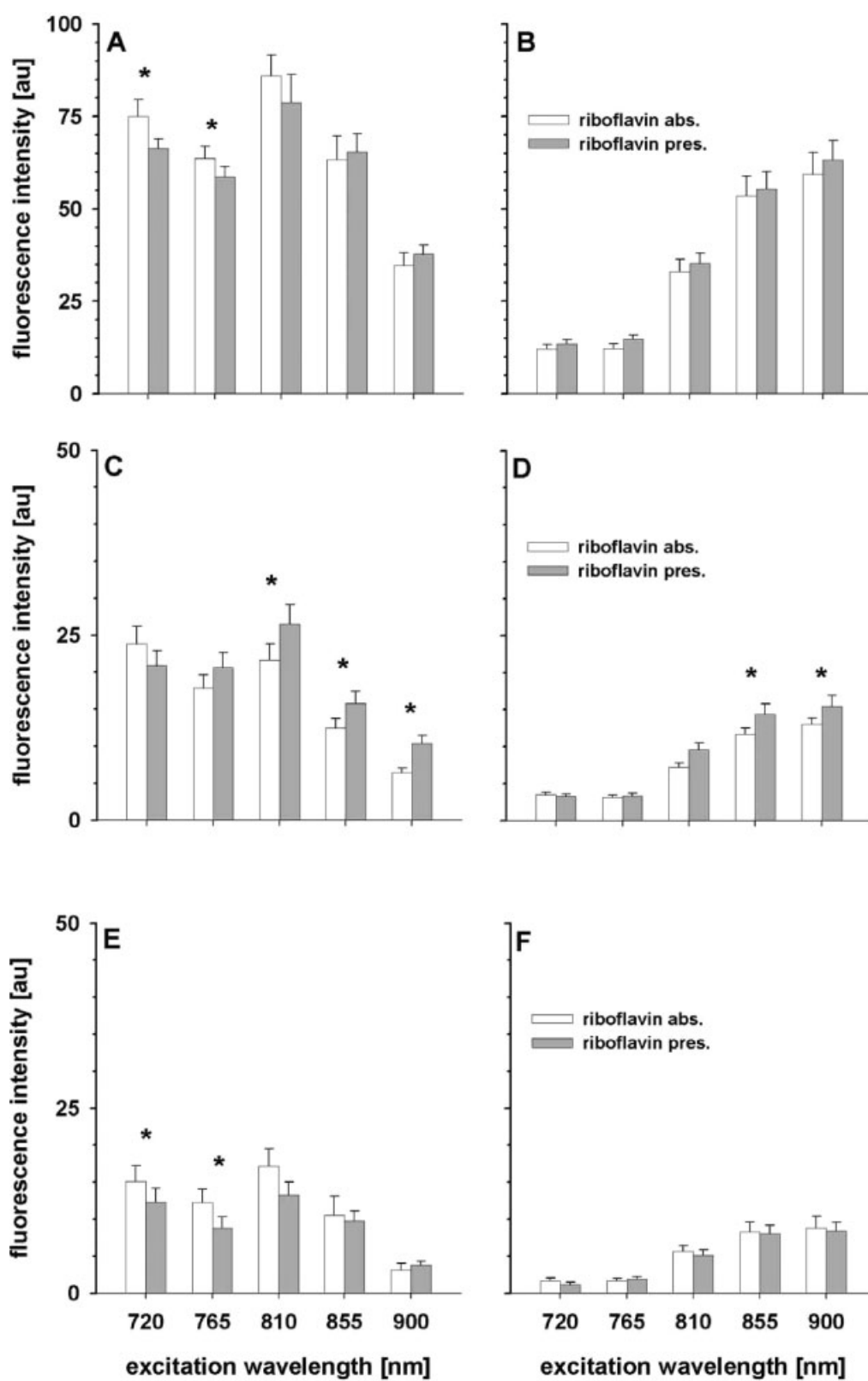


Fig. 7. Change of AF excitation–emission spectrum upon addition of free riboflavin. The AF was detected in the 400- to 490-nm band (A,C,E) and in the 500- to 560-nm band (B,D,F) and excited in two-photon mode using 720-, 765-, 810-, 855-, and 900-nm light. The AF

was registered in the absence (white bars) and presence (gray bars) of riboflavin in the cytoplasm (A,B), at the plasma membrane (C,D), and in the nuclei (E,F) of HepG2 cells. Significant ($P = 0.05$) AF changes are indicated with asterisks.

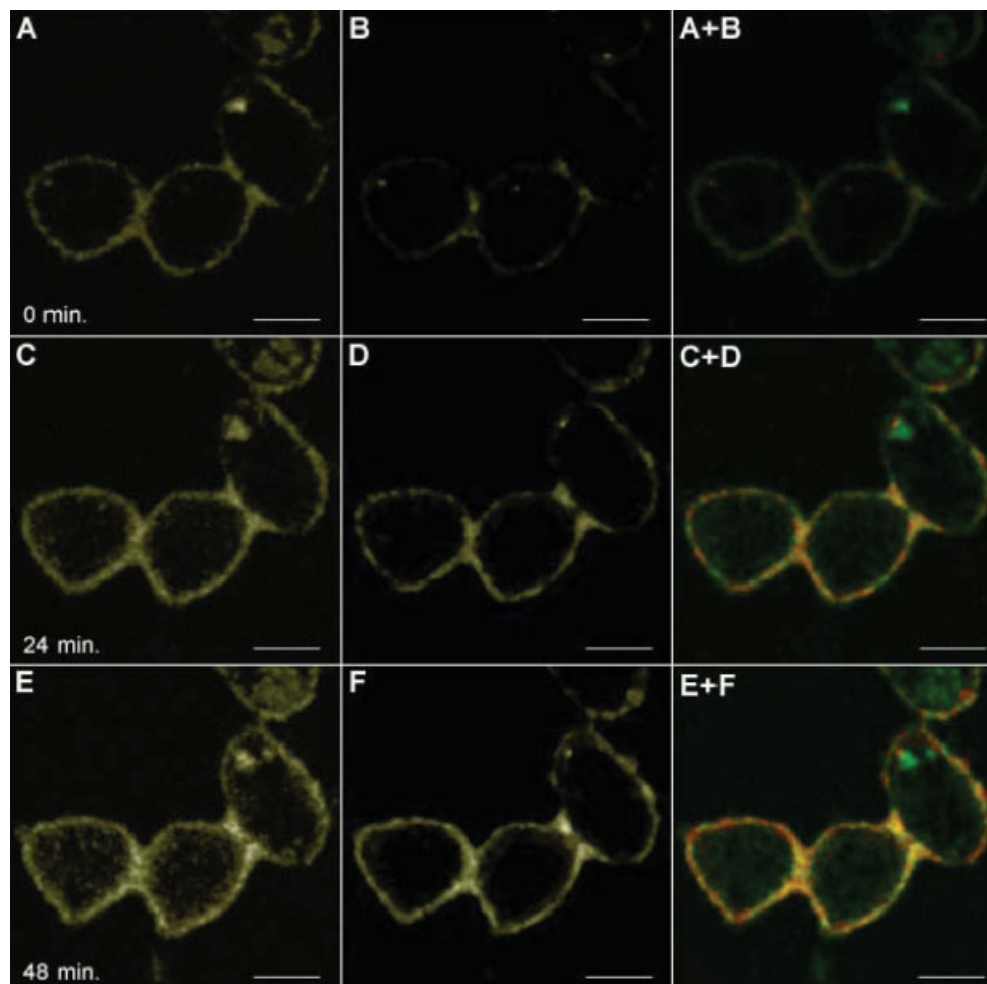


Fig. 8. Increase of green AF in HepG2 cells incubated with an exogenous electron acceptor, CTC. Green AF (A, C, E) was registered in the range of 490–550 nm, red fluorescence (B, D, F) of reduced CTC (CTC-formazan) in the range of 585–630 nm. The images were col-

lected at 0, 24, and 48 min following the addition of CTC. Bar: 10 μ m. [Color figure can be viewed in the online issue, which is available at www.interscience.wiley.com.]

sity of plasma-membrane AF observed with 457-nm excitation. Similarly, treatment with H_2O_2 also had no effect on the membrane AF. However, we observed that cytoplasm AF intensity increased after treatment with H_2O_2 , whereas incubation with a strong reductant sodium dithionite solution caused decrease of the overall AF both in living and in fixed cells (data not shown).

DISCUSSION

Our data indicate that AF of HepG2 cells is a complex phenomenon and depends on the excitation wavelength and on the cell metabolic state. Furthermore, AF varies among subcellular compartments. When maintained in optimal growth conditions and excited with violet light, the cells exhibit green AF associated with plasma membranes, as demonstrated by colocalization with DiIC18. One should note, however, that the thickness of plasma membranes is estimated to be in the order of 10 nm. Thus, owing to the fact that spatial resolution of the registered images was not higher than 250 nm, it was not possible to establish whether

the AF originated from the internal side of the membrane, from its interior or from the external side.

The fact that the fluorophore responsible for AF was not able to diffuse rapidly along the lipid phase of plasma membranes indicates that the fluorophore may be closely associated with a plasma membrane protein and be anchored to the underlying cytoskeleton. This notion is in agreement with the fact that compromising the membrane integrity does not lead to immediate loss of plasma-membrane AF. One may note that these results agree with observations reported by others (Nokubo et al., 1988).

The spectral data presented do not have sufficient resolution to precisely identify the plasma-membrane fluorophore(s). Nonetheless, the excitation/emission characteristics of the membrane AF indicate that it may originate from a flavin derivative. FAD, FMN, and riboflavin are likely candidates. Owing to the fact that fluorescence spectra of these fluorochromes overlap closely one may not distinguish them using microscope techniques. AF of flavoproteins in mitochondria of various cell types has been reported in several papers (Pat-

terson et al., 2000; Rocheleau et al., 2004). One may note that spectral characteristics of plasma membrane AF for HepG2 cells match those of mitochondrial AF when excitation and detection bands are optimized for flavins. On the other hand, when excitation and detection are performed at shorter wavelengths, the spectra of mitochondria and plasma membrane differ. This fact is in agreement with reports indicating that reduced pyridine nucleotides (NADH and NADPH) may contribute to mitochondrial AF together with flavoproteins (Croce et al., 2004; Patterson et al., 2000; Rocheleau et al., 2004).

Several explanations for the presence of plasma membrane AF may be put forward. It has been postulated that membrane AF was due to the presence of riboflavin transported to cells (Lowy and Spring, 1990). However, it is difficult to understand how a constant concentration of free riboflavin would be maintained by the cell in the region close to the plasma membrane. Kinetic studies and examination of riboflavin transport into the cell reported by others do not support the existence of any riboflavin "repository" in the region of the plasma membrane (Said et al., 1998).

It is more probable that the AF originated from a cofactor of an enzyme bound to the plasma membrane. An oxidoreductase which contains FMN or FAD as a cofactor seems a likely candidate for such enzyme. The biological significance of cell-surface NADPH oxidoreductases (ECTO-NOX) in various cell types has been recently recognized and documented (Berridge and Tan, 2000; Morre and Morre, 2003; Scarlett et al., 2005). Apart from the well-known role of the trans-plasma-membrane electron-transport systems in cellular defense, these enzymes, identified in many living cells, regulate processes such as redox homeostasis, and control cell growth and survival (Baker et al., 2004). The spectral signature of plasma-membrane AF reported here and the anchoring of the fluorochrome in the plasma membrane are in agreement with this hypothesis. Furthermore, the increase of the plasma-membrane AF upon reduction of an exogenous electron may be explained by oxidation of the flavin cofactor of this putative enzyme. The reductive activity associated with the plasma membrane of HepG2 cells has previously been demonstrated by us using a nitroxide spin probe as an electron acceptor (Bernas and Dobrucki, 1998).

The practical importance of the reported AF is that the green fluorescence detected in plasma membranes of viable, intact as well as of fixed hepatocytes is sufficiently strong to be a sizable but unwanted component of signals from any other green-emitting dye recorded by flow or image cytometry. As the described AF is spectrally similar to fluorescein and is not uniform all over the cell body, care must be taken in order not to confuse it with surface binding of fluorescein-tagged antibodies. Plasma-membrane AF may also be a meaningful biological parameter providing information about viability, plasma membrane integrity, or redox state. Those applications need further investigation.

ACKNOWLEDGMENTS

We thank Prof. Z. Zak of Jagiellonian University, Krakow, for interesting discussions, and Mrs Barbara Czuba-Pelech, Eng., for skillful technical assistance.

REFERENCES

- Andersson H, Baechi T, Hoechl M, Richter C. 1998. Autofluorescence of living cells. *J Microsc* 191 (Part 1):1–7.
- Aubin JE. 1979. Autofluorescence of viable cultured mammalian cells. *J Histochem Cytochem* 27:36–43.
- Baker MA, Lane DJR, Ly JD, De Pinto V, Lawen A. 2004. VDAC1 is a transplasma membrane NADH-ferricyanide reductase. *J Biol Chem* 279:4811–4819.
- Bennett BD, Jetton TL, Ying G, Magnuson MA, Piston DW. 1996. Quantitative subcellular imaging of glucose metabolism within intact pancreatic islets. *J Biol Chem* 271:3647–3651.
- Benson RC, Meyer RA, Zaruba ME, McKhann GM. 1979. Cellular autofluorescence—Is it due to flavins? *J Histochem Cytochem* 27:44–48.
- Bernas T, Dobrucki J. 1998. Extracellular reduction of Cat1 free radical by transformed human hepatocytes. *Biosci Rep* 18:341–350.
- Bernas T, Dobrucki J. 1999. Reduction of a tetrazolium salt, CTC, by intact HepG2 human hepatoma cells: Subcellular localisation of reducing systems. *Biochim Biophys Acta* 1451:73–81.
- Berridge MV, Tan AS. 2000. Cell-surface NAD(P)H-oxidase: Relationship to trans-plasma membrane NADH-oxidoreductase and a potential source of circulating NADH-oxidase. *Antioxid Redox Signal* 2:277–288.
- Bondza-Kibangou P, Millot C, Dufer J, Millot JM. 2001. Microspectrofluorometry of autofluorescence emission from human leukemic living cells under oxidative stress. *Biol Cell* 93:273–280.
- Brookner CK, Follen M, Boiko I, Galvan J, Thomsen S, Malpica A, Suzuki S, Lotan R, Richards-Kortum R. 2000. Autofluorescence patterns in short-term cultures of normal cervical tissue. *Photochem Photobiol* 71:730–736.
- Croce AC, Spano A, Locatelli D, Barni S, Sciola L, Bottiroli G. 1999. Dependence of fibroblast autofluorescence properties on normal and transformed conditions. Role of the metabolic activity. *Photochem Photobiol* 69:364–374.
- Croce AC, Ferrigno A, Vairetti M, Bertone R, Freitas I, Bottiroli G. 2004. Autofluorescence properties of isolated rat hepatocytes under different metabolic conditions. *Photochem Photobiol Sci* 3:920–926.
- DaCosta RS, Andersson H, Cirocco M, Marcon NE, Wilson BC. 2005. Autofluorescence characterisation of isolated whole crypts and primary cultured human epithelial cells from normal, hyperplastic, and adenomatous colonic mucosa. *J Clin Pathol* 58:766–774.
- Dellinger M, Geze M, Santus R, Kohen E, Kohen C, Hirschberg JG, Monti M. 1998. Imaging of cells by autofluorescence: A new tool in the probing of biopharmaceutical effects at the intracellular level. *Biotechnol Appl Biochem* 28 (Part 1):25–32.
- Eng J, Lynch RM, Balaban RS. 1989. Nicotinamide adenine dinucleotide fluorescence spectroscopy and imaging of isolated cardiac myocytes. *Biophys J* 55:621–630.
- Georgakoudi I, Jacobson BC, Muller MG, Sheets EE, Badizadegan K, Carr-Locke DL, Crum CP, Boone CW, Dasari RR, Van Dam J, Feld MS. 2002. NAD(P)H and collagen as *in vivo* quantitative fluorescent biomarkers of epithelial precancerous changes. *Cancer Res* 62:682–687.
- Huang S, Heikal AA, Webb WW. 2002. Two-photon fluorescence spectroscopy and microscopy of NAD(P)H and flavoprotein. *Biophys J* 82:2811–2825.
- Huang Z, Zheng W, Xie S, Chen R, Zeng H, McLean DI, Lui H. 2004. Laser-induced autofluorescence microscopy of normal and tumor human colonic tissue. *Int J Oncol* 24:59–63.
- Kara M, DaCosta RS, Wilson BC, Marcon NE, Bergman J. 2004. Autofluorescence-based detection of early neoplasia in patients with Barrett's esophagus. *Dig Dis* 22:134–141.
- Kuznetsov AV, Mayboroda O, Kunz D, Winkler K, Schubert W, Kunz WS. 1998. Functional imaging of mitochondria in saponin-permeabilized mice muscle fibers. *J Cell Biol* 140:1091–1099.
- Lowy RJ, Spring KR. 1990. Identification of riboflavin transport by MDCK cells using quantitative fluorescence video microscopy. *J Membr Biol* 117:91–99.
- Masters BR, Chance B. 1999. Redox confocal imaging: Intrinsic fluorescence probes of cellular metabolism. In: Mason WT, editor. *Fluorescent and luminescent probes for biological activity. A practical guide to technology for quantitative real-time analysis*. San Diego, CA: Academic Press.
- Matsui H, Murata Y, Hirano K, Sasaki T, Shiba R, Muto H, Ohno T. 1998. Hydrogen peroxide-induced cellular injury is associated with increase in endogenous fluorescence from rat gastric mucosal epithelial cell culture: A new method for detecting oxidative cellular injury by fluorescence measurement. *J Gastroenterol* 33:318–325.
- Mayeno AN, Hamann KJ, Gleich GJ. 1992. Granule-associated flavin adenine dinucleotide (FAD) is responsible for eosinophil autofluorescence. *J Leukoc Biol* 51:172–175.

- Morre DJ, Morre DM. 2003. Cell surface NADH oxidases (ECTO-NOX proteins) with roles in cancer, cellular time-keeping, growth, aging and neurodegenerative diseases. *Free Radic Res* 37:795–808.
- Nokubo M, Nagy I, Kitani K, Ohta M. 1988. Characterization of the autofluorescence of rat liver plasma membranes. *Biochim Biophys Acta* 939:441–448.
- Nokubo M, Ohta M, Kitani K, Nagy I. 1989. Identification of protein-bound riboflavin in rat hepatocyte plasma membrane as a source of autofluorescence. *Biochim Biophys Acta* 981:303–308.
- Patterson GH, Knobel SM, Arkhammar P, Thastrup O, Piston DW. 2000. Separation of the glucose-stimulated cytoplasmic and mitochondrial NAD(P)H responses in pancreatic islet β cells. *Proc Natl Acad Sci USA* 97:5203–5207.
- Piston DW, Masters BR, Webb WW. 1995. Three-dimensionally resolved NAD(P)H cellular metabolic redox imaging of the in situ cornea with two-photon excitation laser scanning microscopy. *J Microsc* 178 (Part 1):20–27.
- Plettenberg HK, Hoffmann M. 2002. Applications of autofluorescence for characterisation of biological systems (biomonitoring). *Biomed Tech (Berl)* 47 (Suppl 1, Part 2):596–597.
- Puppels GJ, Coremans JMCC, Bruining HA. 1999. In vivo semiquantitative NADPH fluorescence imaging. In: Mason WT, editor. *Fluorescent and luminescent probes for biological activity. A practical guide to technology for quantitative real-time analysis*. San Diego, CA: Academic Press.
- Reinert KC, Dunbar RL, Gao W, Chen G, Ebner TJ. 2004. Flavoprotein autofluorescence imaging of neuronal activation in the cerebral cortex in vivo. *J Neurophysiol* 92:199–211.
- Rocheleau JV, Head WS, Nicholson WE, Powers AC, Piston DW. 2002. Pancreatic islet β cells transiently metabolize pyruvate. *J Biol Chem* 277:30914–30920.
- Rocheleau JV, Head WS, Piston DW. 2004. Quantitative NAD(P)H/flavoprotein autofluorescence imaging reveals metabolic mechanisms of pancreatic islet pyruvate response. *J Biol Chem* 279:31780–31787.
- Said HM, Ortiz A, Ma TY, McCloud E. 1998. Riboflavin uptake by the human-derived liver cells Hep G2: Mechanism and regulation. *J Cell Physiol* 176:588–594.
- Scarlett DJ, Herst PM, Berridge MV. 2005. Multiple proteins with single activities or a single protein with multiple activities: The conundrum of cell surface NADH oxidoreductases. *Biochim Biophys Acta* 1708:108–119.
- Thorell B. 1983. Flow-cytometric monitoring of intracellular flavins simultaneously with NAD(P)H levels. *Cytometry* 4:61–65.
- Watt SM, Burgess AW, Metcalf D, Battye FL. 1980. Isolation of mouse bone marrow neutrophils by light scatter and autofluorescence. *J Histochem Cytochem* 28:934–946.
- Weil GJ, Chused TM. 1981. Eosinophil autofluorescence and its use in isolation and analysis of human eosinophils using flow microfluorometry. *Blood* 57:1099–1104.